JPhys Materials

PAPER • **OPEN ACCESS**

Radiation-induced effects on commercial 3D printing materials exposed to high x-ray doses

To cite this article: L Sostero *et al* 2025 *J. Phys. Mater.* **8** 035003

Journal of Physics: Materials

PAPER

Radiation-induced effects on commercial 3D printing materials exposed to high x-ray doses

L Sostero[1,2], M Ferrari[3], D Pagano[1,2,*], S Pandini[1], C Pasini[1], A Boukenter[3], A Morana[3] and S Girard[3,4]

[1] Department of Mechanical and Industrial Engineering, University of Brescia, Brescia, Italy
[2] Istituto Nazionale di Fisica Nucleare (INFN), Pavia, Italy
[3] Universite Jean Monnet Saint-Etienne, CNRS, Institut d'Optique Graduate School, Laboratoire Hubert Curien UMR 5516, F-42023 Saint-Etienne, France
[4] Institut Universitaire de France (IUF), Ministere de l'Enseignement Superieur et de la Recherche, sis 1 rue Descartes 75005 Paris, France
[*] Author to whom any correspondence should be addressed.

E-mail: davide.pagano@unibs.it

Keywords: 3D printing, polymers, x-ray, radiation-induced degradation

OPEN ACCESS

RECEIVED
27 December 2024

REVISED
23 April 2025

ACCEPTED FOR PUBLICATION
21 May 2025

PUBLISHED
29 May 2025

Abstract

Fused filament fabrication is among the most widely used 3D printing techniques, that allows to create complex devices from a continuous filament of a polymeric material. This adaptable technique has garnered considerable interest for the development of components functioning under severe radiation environments, including particle accelerators and nuclear reactors. In this work, we evaluated the radiation effects on several categories of commercial printing materials, namely the poly(lactic acid) (PLA), the acrylonitrile butadiene styrene (ABS), and a thermoplastic elastomer (TPE). Printing filaments have been exposed to x-rays (up to 160 keV) at 0.60 Gy s^{-1}, from 45 kGy to 2 MGy. The results from tensile tests, thermal analyses (differential scanning calorimetry, thermogravimetric analysis, dynamic mechanical thermal analysis), and spectroscopy tests (Fourier transform infrared spectroscopy and Raman analysis) reveal a dose-dependent degradation of material properties, predominantly affecting mechanical properties rather than chemical and thermal ones. The PLA shows the lowest radiation tolerance among the three, dramatically decreasing the tensile strength above 100 kGy, while TPE and ABS reach a comparable mechanical degradation after 1 MGy and 2 MGy, respectively. Radiation-induced effects are investigated, and the degradation is primarily attributed to chain scission as the principal damage mechanism.

1. Introduction

Polymeric materials for 3D printing are of increasing interest for the realisation of components operating in extreme radiation conditions, such as particle accelerators, nuclear facilities and repositories for radioactive waste [1, 2], medical field and FLASH therapy [3–5], and space missions [6, 7]. For this reason, radiation effects on several categories of commercial printing materials must be evaluated.

The effect of radiation on polymers depends on various parameters, such as the dose level, the irradiation temperature, the dose rate, and the oxygenation of the sample [8, 9]. The irradiation induces excitations and ionisations of the polymer chains, leading to the formation of free radicals and ions that react, resulting in cross-linking and/or chain scission. The two competing dynamics occur simultaneously, and one is usually dominant depending on the specific polymer and on the irradiation conditions. Cross-linking is related to the formation of new bonds in between the polymer chains, typically leading to an increase of the elastic modulus and strength and to embrittlement of the material. On the contrary, chain scission leads to a reduction in molecular weight and consequent degradation of the mechanical properties of the polymer, usually losing in strength and elongation at break [8, 10].

To the best of our knowledge, the studies on the effect of ionising radiation on polymers for 3D printing are limited to the effect of high energy (>1 MeV) photons irradiation at a dose rate ranging from 0.1 to 150 kGy h^{-1} [6, 10–18], or to 2.5–10 MeV *e*-beam irradiation up to 200 kGy [10, 15, 19, 20]. Moreover, the existing literature on radiation effects in these materials primarily focuses on printed samples. However, as in space applications, for example, the filament may also be exposed to radiation before the printing process. Crucially, the effects on the raw material must be thoroughly assessed, since they reflect the key consequences of irradiation on the printed item. Therefore, a new research activity is being developed to broaden the available knowledge about radiation effects on popular 3D printing materials used for fused filament fabrication, namely the poly(lactic acid) (PLA), the acrylonitrile butadiene styrene (ABS), and a thermoplastic elastomer (TPE).

Printing filaments have been exposed to x-rays (up to 160 keV) at 0.60 Gy s^{-1} (2.16 kGy h^{-1}), from 45 kGy[H_2O] to 2 MGy[H_2O], that are typical dose rate and doses reached in extreme radiation environments such as the ones generated by particle accelerators and fusion facilities [21].

In the following, we show the changes in a selection of properties for the irradiated materials as a function of the dose. The irradiations were performed at the Hubert Curien Laboratory (LabHC) in Saint-Etienne (France), and sample characterisations were jointly performed at LabHC and at the Materials Science and Technology Laboratory of the University of Brescia (Italy). The performed multi-scale investigations include thermal, mechanical and spectroscopical analyses, more precisely the thermogravimetric analysis (TGA), differential scanning calorimetry (DSC), dynamic mechanical thermal analysis (DMTA), tensile test, Fourier transform infrared spectroscopy (FTIR), and Raman spectroscopy, aiming at finding correlations between structural and macroscopic radiation effects.

2. Method

The effects of radiations on 3D printing materials were explored on raw printing filaments of three different materials: PLA (Raise3D Premium, Irvine, CA, USA), ABS (Raise3D Premium ABS, Irvine, CA, USA), and TPE (Bioflex produced by Filoalfa and purchased by Maip Compounding S.r.l., Torino, Italy). PLA is a semi-crystalline polymer [22] which is known for its biodegradability and low distortion level during printing, although it has low mechanical properties and low thermal conductivity [23]. ABS is an amorphous material [24] and it is not considered biodegradable, but it is widely used for its high mechanical properties and chemical resistance [23]. Finally, TPE is a TPE, which is reported to have a segmented structure, composed by two distinct semicrystalline phases [25]. TPE has unique rubber like elasticity, good chemical and solvent resistance, and it is a recyclable material [26].

Samples are shown in figure 1(a) and have a nominal diameter of 1.75 mm. The segments of 10 cm length are prepared for tensile tests and the 3 cm long ones for the other analyses.

2.1. Sample irradiation

The irradiations were performed at the LabHC using commercial x-ray tubes operating at a voltage of 160 kV, and figure 1(b) shows the experimental setup. The dose rate in correspondence to the irradiation positions was measured on a grid of points using a PTW 23 344 compact ionisation chamber—which provides a dose rate to water value—shielded by 1.5 mm of aluminium to reproduce the same irradiation conditions of samples. Surface dose homogeneity in the irradiation position is limited to ± 15%.

Knowing the material of the target in the x-ray tube (tungsten), the anode angle (30°), and the inherent filtration (4 mm of beryllium), the energy spectrum of x-rays emitted by the tube can be estimated using SpekPy v2.0 [27], and it is shown in figure 2(a).

In the experimental setup, samples are placed below an aluminium foil 1.5 mm thick: this filter hardens the spectrum by strongly attenuating photons up to (approximately) 30 keV, as shown in figure 2(a), which would cause a non-negligible dose inhomogeneity in the sample due to their attenuation in the sample thickness. Dose homogeneity is improved at the expense of the dose rate absorbed by the sample, which is reduced by almost a factor of ten in comparison to the unfiltered scenario. Dose-depth curves in the two conditions are reported in figure 2(b). These dose profiles were estimated using Monte Carlo simulations realised by PHITS [28]: the dose was computed in 15 slices of a cylinder of water of 1.75 mm diameter and 30 mm length, exposed to an isotropic source of x-rays, and energy spectrum as figure 2(a).

The irradiated samples have been exposed to a dose rate of 0.60 Gy s^{-1} (2.16 kGy h^{-1}), and doses ranging from 45 kGy to 2 MGy, as reported in table 1. Irradiations were performed at monitored room temperature, and the selected dose rate does not lead to a considerable sample heating. In the present work, all the reported dose values refer to dose to water.

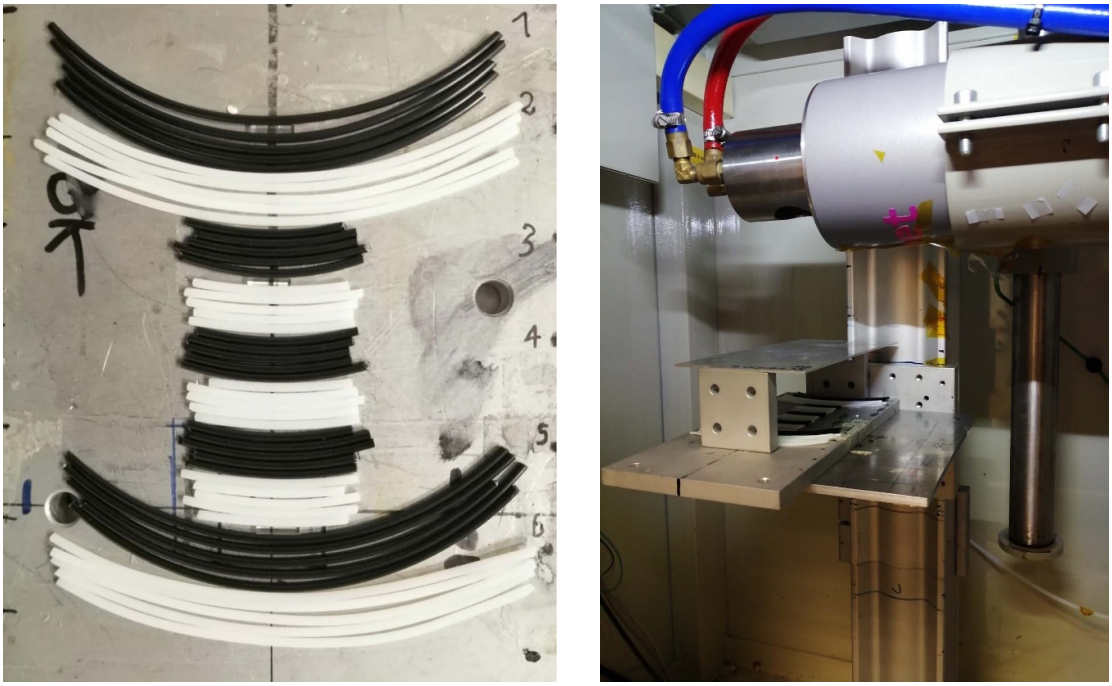

(a) (b)

Figure 1. (a) Raw printing filaments in ABS (black colour) and PLA (white colour), (b) irradiation setup.

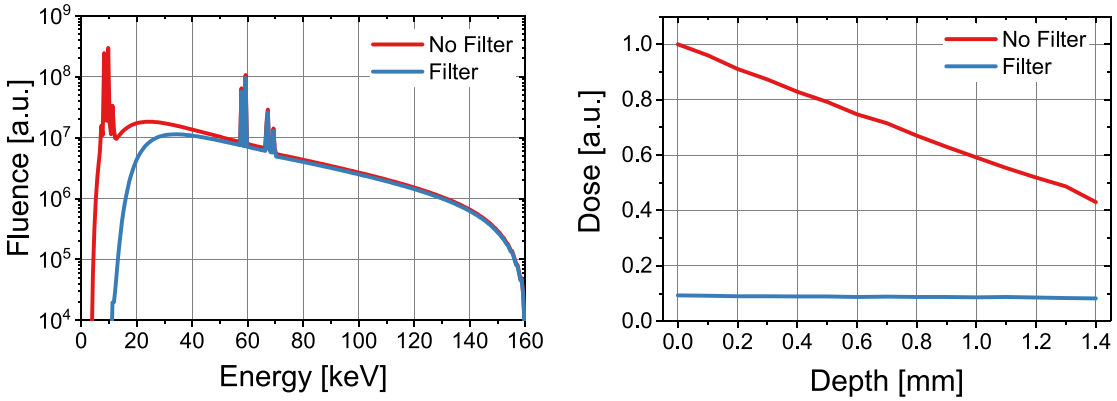

(a) (b)

Figure 2. (a) X-ray energy spectrum from SpekPy [27] and (b) dose profiles in water estimated using PHITS, with and without a 1.5 mm thick aluminium filter.

2.2. Tensile test

The mechanical properties of filaments before and after irradiation were evaluated under tensile conditions at room temperature, by means of an electromechanical dynamometer (model 3366, Instron, MA, US). A crosshead speed of 50 mm min^{-1} and a gauge length of 60 mm were adopted (strain rate of 0.83 min^{-1}). For each material and each dose investigated, tests were repeated on 5 samples. The results were expressed in terms of nominal stress (σ) versus strain (ϵ) curves. From these curves, the following properties were obtained: the Young's modulus (E), evaluated as the initial slope of the curves; the tensile strength (TS), evaluated as the maximum stress (corresponding to the yield point for specimens showing ductile failure and to the ultimate stress for those showing brittle failure); the strain at break (ϵ_b). For specimens that could not reach failure during the tests, it is only possible to indicate that TS and ϵ_b are higher than the last recorded values.

2.3. Thermal tests

The non-irradiated and irradiated specimens were subjected to various thermal and thermo-mechanical characterisations: DSC; TGA; DMTA.

2.3.1. DSC

DSC analyses were carried out by means of a DSC Q100 calorimeter (TA Instruments, New Castle, DE, US) under nitrogen atmosphere (50 ml min^{-1}). Samples of about 10 mg were cut from filaments in their pristine condition and after irradiation. The following thermal program was applied: (i) heating from −80 °C to 280 °C at 10 °C min^{-1}; (ii) cooling from 128 °C to −80 °C at 10 °C min^{-1}; (iii) heating from −80 °C to 280 °C at 10 °C min^{-1}.

2.3.2. TGA

TGA was performed on samples of about 10 mg cut from filaments in their pristine condition and after irradiation, by means of a TGA Q500 analyser (TA Instruments New Castle, DE, US). A heating ramp from room temperature to 700 °C at 10 °C min^{-1} was applied.

2.3.3. DMTA

DMTA was carried out by means of a DMA Q800 analyser (TA Instruments New Castle, DE, US) on small rods cut from the filaments in the pristine condition and after irradiation (overall length: 30 mm ca.; gauge length: 15 mm ca.). Irradiated PLA could not be tested because of excessive embrittlement caused by irradiation. ABS and TPE specimens were tested under dynamic tensile configuration with an applied displacement amplitude equal to 15 μm and a frequency of 1 Hz, while heating them at 3 °C min^{-1} through a temperature range depending on the specific polymer. The initial temperature (room temperature for ABS; −40 °C for TPE) was selected so to start the analyses below the glass transition temperature of the material, while the end of the tests occurred when the specimens elongated above the maximum length allowed by the analyser as, at high temperature, the early stage of the flow regime was approached.

2.4. Spectroscopy tests

FTIR analysis was performed by means of a Thermo Scientific, Nicolet iS50 FTIR spectrophotometer (Thermo Fisher Scientific, Madison, WI, US) equipped with a PIKE MIRacle attenuated total reflectance attachment. The spectra were recorded over a range of 600–4000 cm^{-1}. Raman analysis was performed using an inVia Qontor microscope (Renishaw plc, UK) and a laser wavelength of 442 nm. The spectra were recorded over a range of 500–3500 cm^{-1}. For Raman analysis, samples were cut perpendicular to the sample axis, and the analysis was performed at three points along the radius of the filament on the cutting plane (near the surface, near the centre of the filament and at an intermediate point).

3. Results

3.1. Tensile test results

The mechanical properties of PLA, ABS, and TPE filaments before and after irradiation were evaluated by tensile tests. Figures 3–5 present a selection of stress–strain curves and optical microscope images of the specimens taken at the end of the experiments, highlighting the progressive radiation-induced effect on the mechanical response of the materials. Table 1 shows the tensile properties of the filaments for all the conditions under investigation, ranging from no irradiation to such a high dose that the material becomes too brittle to be clamped and tested at the dynamometer; more specifically, for each material and dose, it reports the measured values of Young's modulus (E), TS, and strain at break (ϵ_b).

The PLA filament exhibits a remarkable degradation of the mechanical properties after irradiation. For the pristine material, PLA stress–strain curves (figure 3(a)) show a transition from an initial linear elastic response to a stress peak followed by a plateau, indicating the accumulation of plastic deformation. During the latter phase, the specimen forms a neck that becomes progressively thinner until it breaks, as clearly visible in figures 3(c) and (f). By contrast, even at the lowest explored dose (45 kGy) the specimens are severely embrittled, as shown by the stress–strain curves (figure 3(b)) and by the appearance of the samples after failure (see the absence of necking or other clear signs of yielding in figures 3(d) and (f)). E and TS are reduced by about 15%–20% in comparison to the non-irradiated value, while ϵ_b decreases by almost one order of magnitude, as reported in table 1. When the dose is increased (144 kGy, see figures 3(e) and (f)), the material embrittlement is so strong that the specimens break while trying to clamp them.

The tensile properties of the ABS filament present negligible changes for dose values up to 300 kGy, whereas significant alterations are measured at the highest doses (1–2 MGy). The stress–strain curves of the specimens irradiated at 292 kGy (figure 4(b)) are comparable to those of the pristine material (figure 4(a)),

Table 1. Mechanical properties under tension for PLA, ABS, and TPE filaments tested in their pristine condition and after irradiation with various dose values: Young's modulus (E), tensile strength (TS), and strain at break (ϵ_b).

Filament	Dose (kGy)	E (MPa)	TS (MPa)	ϵ_b (%)
PLA	0	1960 ± 160	53.2 ± 0.6	33 ± 16
	45	1580 ± 200	45.5 ± 0.4	4.5 ± 0.3
	144	n.a. (too brittle to be tested)		
ABS	0	1470 ± 100	46.0 ± 0.2	31 ± 10
	45	1560 ± 90	43.5 ± 0.5	24 ± 4
	100	1620 ± 190	43.6 ± 1.1	12 ± 7
	139	1460 ± 200	43.7 ± 0.8	32 ± 10
	168	1520 ± 50	47.1 ± 0.3	26 ± 9
	251	1680 ± 50	47.6 ± 0.7	15 ± 3
	292	1470 ± 180	44.8 ± 0.2	21 ± 9
	992	1630 ± 250	30.1 ± 8.2	2 ± 1
	1900	n.a. (too brittle to be tested)		
TPE	0	33.3 ± 1.4	> 12[a]	> 800[a]
	45	31.9 ± 1.6	> 12[a]	> 800[a]
	100	32.6 ± 1.4	> 12[a]	> 800[a]
	139	29.3 ± 0.6	> 12[a]	> 800[a]
	168	33.1 ± 1.0	> 12[a]	> 800[a]
	251	30.8 ± 1.0	6.4 ± 0.3	250 ± 50
	292	27.8 ± 0.7	4.0 ± 0.1	43 ± 3
	910	n.a. (too brittle to be tested)		
	992	20.8 ± 0.3	2.2 ± 0.1	35 ± 3

[a] failure could not be reached

showing a ductile behaviour with a linear elastic region until the characteristic yield stress peak, followed by a strain-softening region and a final plateau. By visual inspection, the broken specimens present multiple white marks perpendicular to the load direction (figure 4(g)), which can be ascribed to yielding phenomena. The more ductile the behaviour, the more these white marks extend throughout the whole cross-section of the specimens; in fact, the fractured surface of non-irradiated ABS has completely changed colour (figure 4(d)), while that of ABS irradiated with 292 kGy (figure 4(e)) is not fully white. On the other hand, at a dose of about 1 MGy (992 kGy, see figures 4(e)–(g)) the ductility of the ABS filament is compromised, exhibiting stress–strain curves that are typical of brittle materials and no signs of yielding (see figure 4(c)). Finally, the dramatic embrittlement observed in ABS after a dose of 1900 kGy prevents the possibility of testing the specimens, due to damages created during clamping.

In order to better quantify the described effects, the values of E, TS and ϵ_b in table 1 can be compared. Irradiation up to 300 kGy causes no significant alterations with respect to the properties of the pristine filament. A slight decrease of ϵ_b may occur, but the values remain overall comparable, given the high values found for the standard deviation. At a higher dose of 1 MGy, TS is reduced by about one third and ϵ_b by about one order of magnitude with respect to the corresponding initial values, while E remains constant.

Finally, the effects of x-rays on the mechanical properties of the TPE filament can be observed for dose values of 250 kGy and higher. It is noteworthy that, for lower dose values, the TPE is able to be deformed at strain values exceeding 800%, without fracture. The test could not continue at higher strain values due to difficulties in keeping the specimen adequately gripped. The stress–strain curves show a nonlinear elastic behaviour with a first region with higher slope followed by a knee that marks the transition to a second region with lower slope (figure 5(a)). The specimen surface appears smooth both before and after testing (figure 5(d)). For doses around 250–300 kGy, the curves present a similar shape, (figure 5(b)), but eventually the specimens are observed to break, starting from cracks that seem to initiate on the surface, so lower strain values are reported. Some of these cracks can be identified on the surface of the tested specimens (figure 5(f)), whereas no cracks are visible at the optical microscope after irradiation before testing (see figure 5(e)). Conversely, specimens irradiated with a dose approaching 1 MGy exhibit a visible repetitive pattern of cracks even after irradiation but before testing (see figure 5(g)), and they break at remarkably lower values of stress and strain (figure 5(c)). Moreover, it is possible to recognise a less shiny outer portion in the cross-sections of the specimens that reached failure, as a further marker of the location where cracks initiate (figure 5(i)). Though the appearance of pores and cracks on irradiated elastomers has been reported in literature for some rubbers exposed to high dose [29], the peculiar pattern here observed is hypothetically ascribed to a combined effect of irradiation and residual stresses accumulated in the filament during its production.

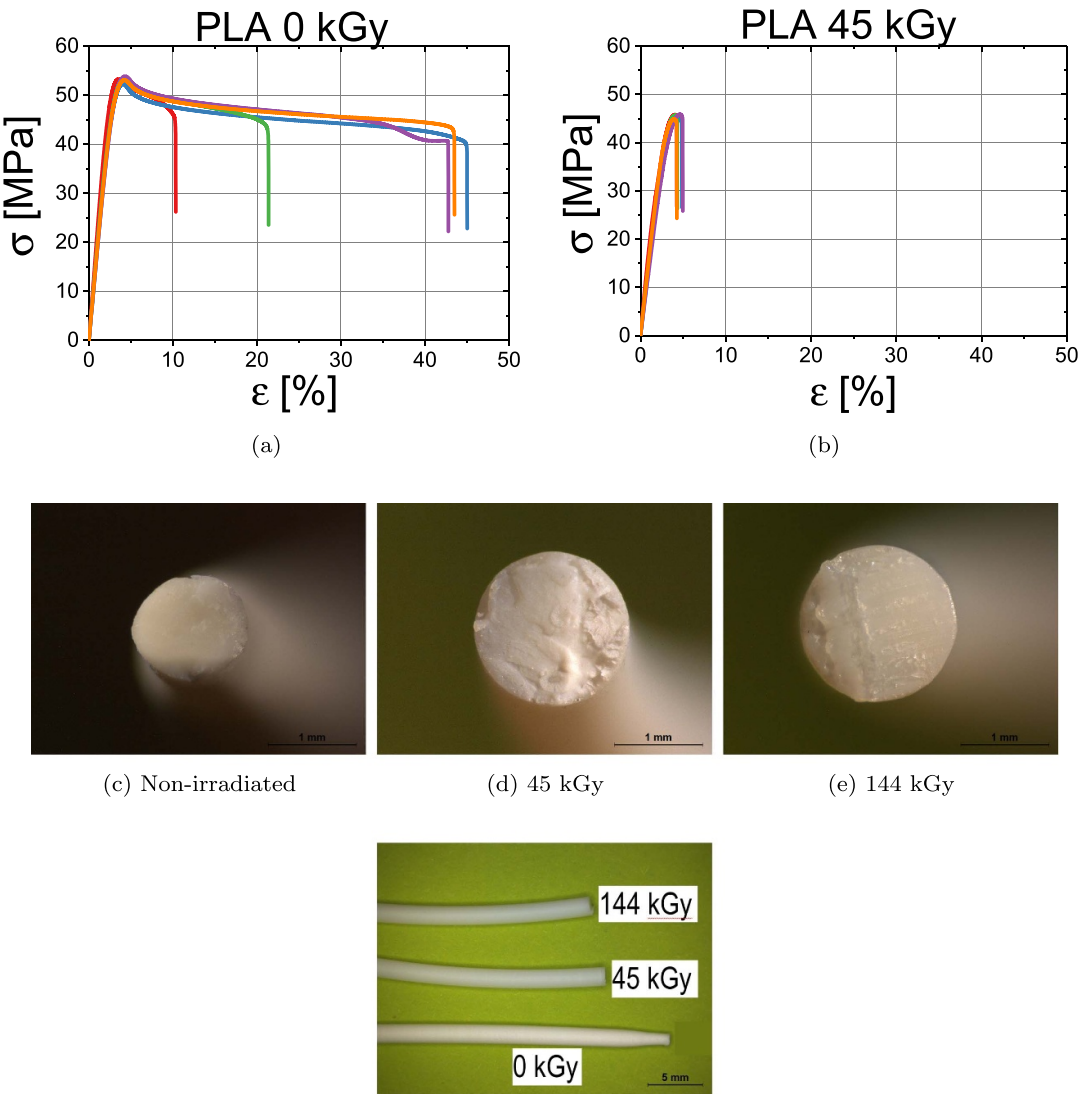

(a) (b)

(c) Non-irradiated (d) 45 kGy (e) 144 kGy

(f) Side view

Figure 3. Tensile test results for PLA filaments tested in their pristine condition and after irradiation with different dose values, selected so to highlight the progressive embrittlement induced by x-rays: (a) and (b) stress–strain curves (each curve corresponds to one of the five samples exposed to the same dose); (c)–(f) optical microscope images of the specimens after the tests. Tensile test on the samples irradiated at 144 kGy was not possible.

Further details on the evolution of the TPE stiffness, strength, and ductility are provided in table 1. No significant changes in E are observed for dose values up to at least 250 kGy, and the stiffness reduction measured at higher doses is likely to be ascribed to the remarkable alteration in the specimen shape when cracks are clearly visible. On the other hand, a progressive decrease in TS and ϵ_b is well manifest as more dose is absorbed. Specimens irradiated at dose values below 200 kGy reach stress values exceeding 12 MPa and strain values above 800%, whereas at a dose of 250 kGy TS falls below 6 MPa and ϵ_b below 250%. At higher doses further damage is reported, until, at doses approaching 1 MGy, specimens may become too brittle to be tested. Here, the batches of specimens irradiated with 910 kGy and with 992 kGy were both extremely embrittled, and only the latter could be tested (TS $\approx$ 2 MPa; $\epsilon_b \approx$ 35%).

3.2. Results of the thermal and thermo-mechanical characterisation

A complete thermal characterisation, including DSC, TGA, and DMTA on both non-irradiated and irradiated specimens, was conducted to integrate the knowledge of material changes due to irradiation. Each technique aimed at elucidating possible variations in the characteristic signals of the examined filaments: specifically, DSC sought to identify changes in the materials characteristic temperatures (glass transition temperature, T_g; melting temperature, T_m; cold crystallisation temperature, T_{cc}) and melting enthalpy (ΔH_m); TGA aimed to evidence variations in the overall thermal degradation process, focusing on the onset and peak temperatures (T_{onset} and T_{peak}, respectively); finally, DMTA was conducted to reveal potential

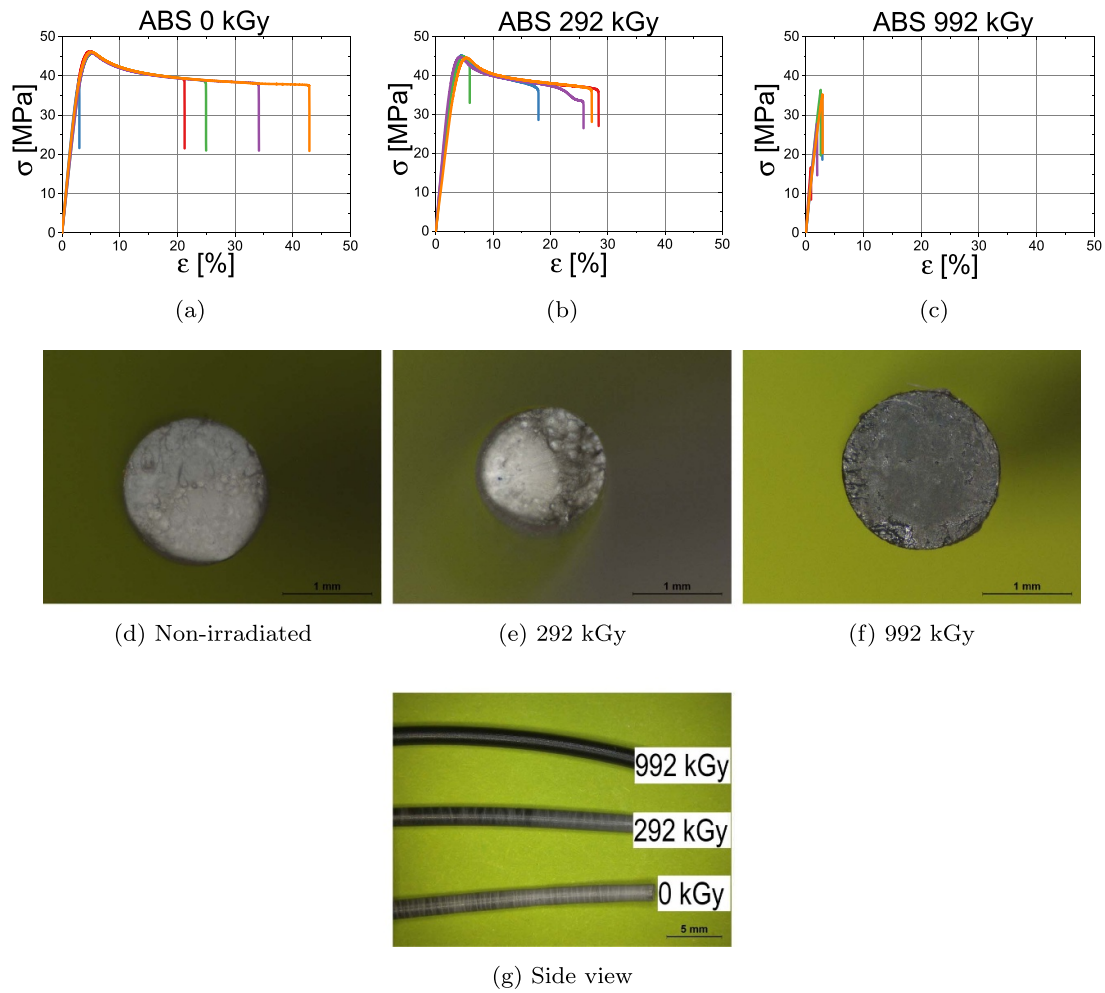

Figure 4. Tensile test results for ABS filaments tested in their pristine condition and after irradiation with different dose values, selected so to highlight the progressive embrittlement induced by x-rays: (a)–(c) stress–strain curves (each curve corresponds to one of the five samples exposed to the same dose); (d)–(g) optical microscope images of the specimens after the tests.

differences in the material's mechanical response as a function of temperature, including alterations in the glass transition temperature and variations in mechanical properties across the glassy, transition, rubbery, and flow regimes.

The outcomes of DSC and TGA analyses on PLA are presented in figures 6(a) and (b), respectively; DMTA could not be performed on irradiated PLA since specimens consistently fractured when secured in the analyser's tensile grips. Despite the significant mechanical embrittlement observed in the PLA specimens investigated, thermal examination provides minimal insights on alterations in these semicrystalline systems. The DSC results, presented here as second heating scans, indicate that non-irradiated and mildly irradiated (45 kGy) specimens exhibit analogous behaviour as the temperature rises, experiencing initial recrystallisation followed by melting, with comparable values for the glass transition temperature (T_g), cold crystallisation temperature (T_{cc}), and melting temperature (T_m, determined at the highest endothermal peak), as detailed in table 2. Only the system irradiated at the highest dose (144 kGy) exhibited significant variations, consisting of a reduction in T_g of almost 20 °C and in T_m of about 10 °C, a modest decline in crystallinity (as suggested by the slight decrease in ΔH_m), and the absence of the cold crystallisation peak. TGA traces indicate a minimal decrease in the temperature at which degradation initiates (T_{onset} in table 2), correlating with the absorbed dose; however, the overall degradation process and the peak temperature, T_{peak}, remain substantially unchanged.

DSC and TGA traces provide minimal insights into the structural evolution of ABS, as illustrated in figures 7(a) and (b), respectively. The DSC curves are those typical of an amorphous polymer and remain almost unchanged, and the glass transition temperature appears to be unaffected by radiation, as shown in table 3. Analogous to the observations made for PLA, the TGA curves indicate that the degradation process remains mainly unaltered upon irradiation; no significant variations are found for doses up to 300 kGy, whereas a slight decrease of both the onset and peak temperature of the degradation process is observed for

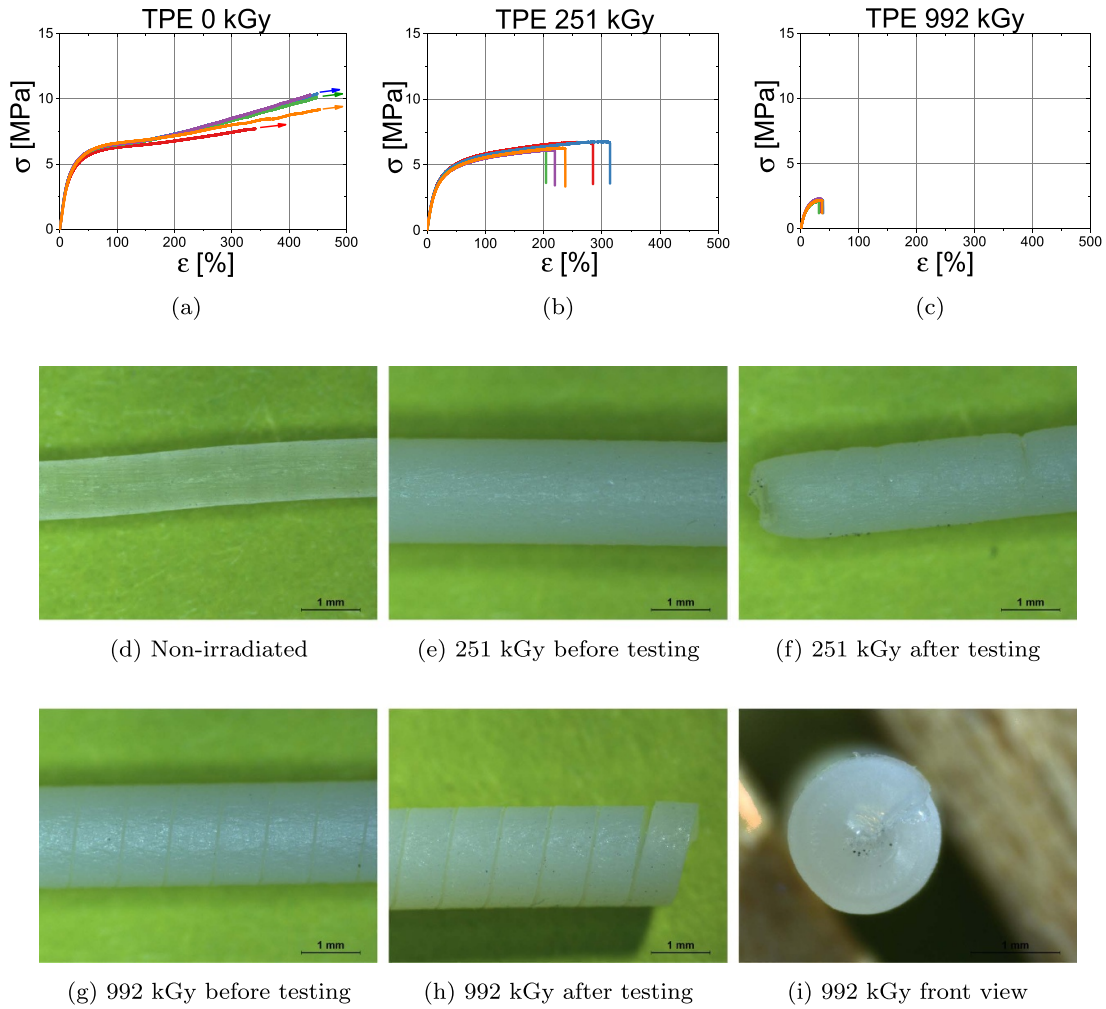

Figure 5. Tensile test results for TPE filaments tested in their pristine condition and after irradiation with different dose values, selected so to highlight the progressive embrittlement induced by x-rays (each curve corresponds to one of the five samples exposed to the same dose): (a)–(c) stress–strain curves; (d)–(g) optical microscope images of the specimens after the tests.

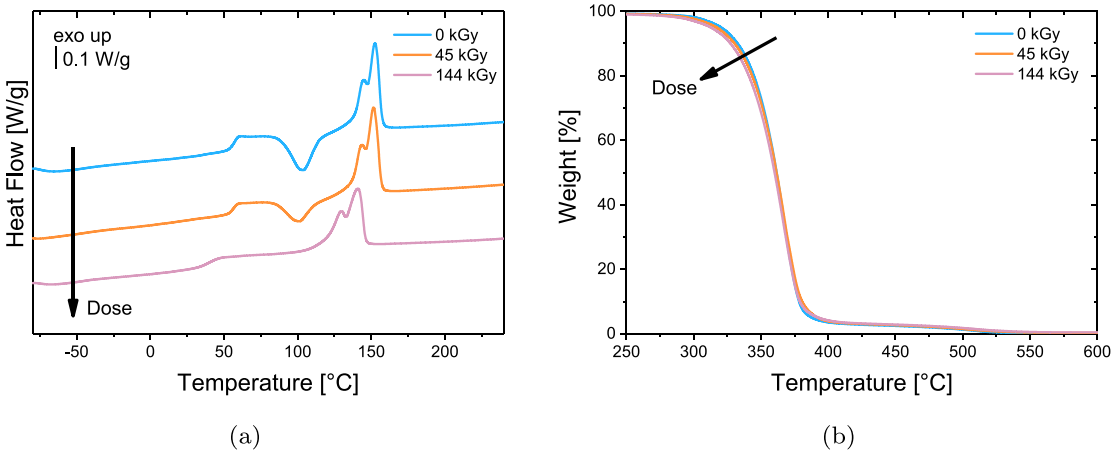

Figure 6. (a) DSC traces (second heating scan) and (b) TGA traces of PLA specimens, non-irradiated and subjected to various x-ray doses.

the most irradiated systems (990 kGy and 1990 kGy), the reduction being more pronounced as the dose increases (table 3).

The storage modulus curves of ABS filaments, obtained by DMTA and presented in figure 7(c), encompass the whole evolution of the mechanical behaviour of the material as the temperature increases.

Table 2. Effect of the irradiation condition on DSC results (from second heating scan) and TGA results for variously irradiated PLA specimens.

	DSC (2nd heating scan)				TGA	
Dose (kGy)	T_g (°C)	T_{cc} (°C)	T_m (°C)	ΔH_m (J g^{-1})	T_{onset} (°C)	T_{peak} (°C)
0	57.4	104	152.7	28.51	309.8	366.9
45	56.4	101.4	151.5	27.79	305.6	366.9
144	39.4	—	141	26.67	300	366.4

Table 3. Effect of the irradiation condition on DSC (from second heating scan), TGA and DMTA results for non-irradiated and variously irradiated ABS specimens (*: could not be tested due to severe embrittlement).

	DSC (2nd heating scan)	TGA		DMTA
Dose (kGy)	T_g (°C)	T_{onset} (°C)	T_{peak} (°C)	T_{flow} (°C)
0	97.5	354.6	415.4	205
45	102.1	359.1	417.8	195
100	98.7	353.7	413.7	190
139	97.9	349.3	411.8	181
168	99.3	354.2	413.8	179
251	98.8	350.8	414.6	173
292	97.6	357.4	416.9	179
992	101.7	343.7	409.3	171
1900	101.6	324.2	403.2	-*

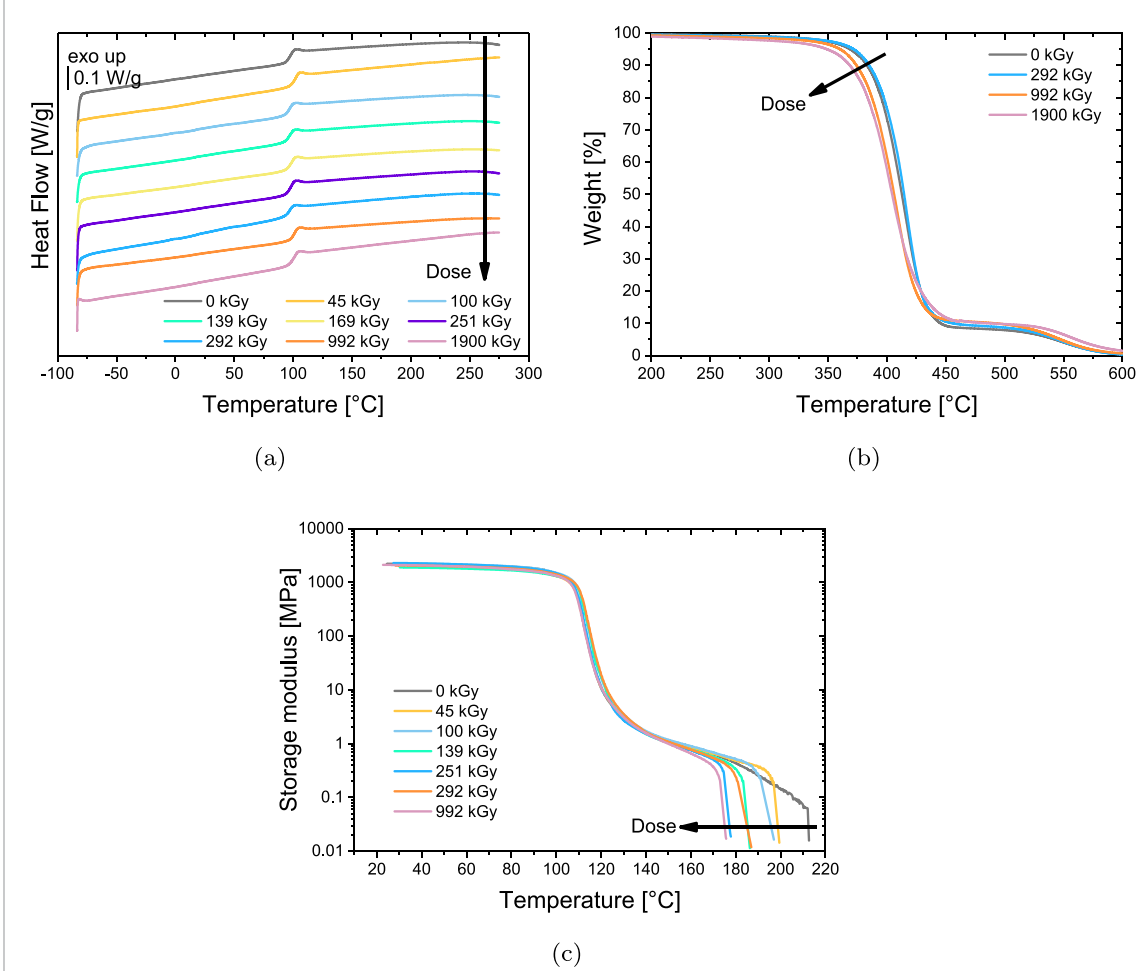

Figure 7. (a) DSC traces (2nd heating scan), (b) TGA traces, and (c) DMTA storage modulus traces for ABS specimens, non-irradiated and subjected to various x-ray doses.

Table 4. Effect of the irradiation condition on DSC (from first and second heating scans), TGA and DMTA results for non-irradiated and variously irradiated TPE specimens.

	DSC						TGA		DMTA
	1st heating scan		2nd heating scan						
Dose (kGy)	T_{exo} (°C)	ΔH_{exo} (J g^{-1})	T_{m1} (°C)	ΔH_{m1} (J g^{-1})	T_{m2} (°C)	ΔH_{m2} (J g^{-1})	T_{onset} (°C)	T_{peak} (°C)	T_{flow} (°C)
0	236.5	13.3	5.7	18.6	189.3	11.9	212.2	350.9	159
45	222.3	10.5	8.5	16.7	189.9	11.3	200.2	341.4	159
100	213.9	5.3	11.2	18.7	191	10.6	177.4	378.4	158
139	185.5	4.9	11	18.8	188.6	9.9	167.5	367.7	154
168	187.4	12.1	14.5	22.4	190.4	13.4	163.7	359.1	152
251	169.7	40.2	13.7	23.2	186.8	14.3	152.3	374.2	151
292	168.3	46.7	13.4	20.6	185.8	12.6	147.4	389.9	150
910	155.9	71.2	2.9	12.5	164.6	8.3	143.1	388.5	128
992	154.5	70.7	5.2	16.5	167.7	11.2	123.1	390.2	139

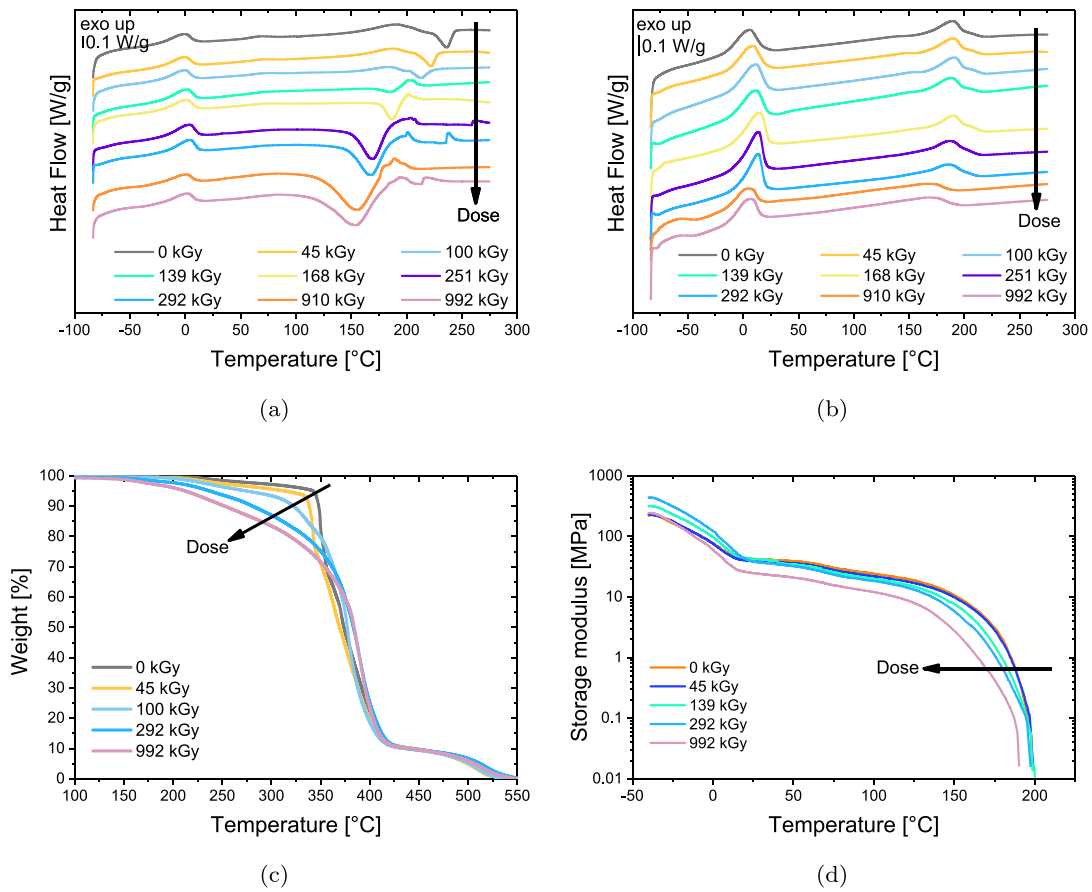

Figure 8. DSC traces (a) first and (b) second heating scan, (c) TGA traces, and (d) DMTA storage modulus traces for TPE specimens, non-irradiated and subjected to various x-ray doses.

The storage modulus ranges from higher values in the glassy plateau, through the glass transition region, to lower values in the rubbery plateau, ultimately transitioning into the flow regime, as indicated by the final downward deviation of the storage modulus. The material evolution from the glassy to the rubbery plateau remains practically unaltered for all specimens, corroborating the findings from DSC. Conversely, irradiation has a visible impact on the final portion of the curves, indicating an entrance in the flow regime that occurs at lower temperatures as the absorbed dose increases. The temperature at which the storage modulus deviates from the rubbery plateau is reported in table 3 as T_{flow}, and undergoes a gradual decrease with the absorbed dose, reaching a reduction of more than 30 °C for irradiation levels around 1 MGy; the highest dose applied (almost 2 MGy) caused such pronounced embrittlement that specimen testing was precluded.

Finally, in the case of TPE, DSC results show a pronounced exothermal anomaly in the first heating scan (figure 8(a)), which disappears in the subsequent heating scan (figure 8(b)), displaying only the melting signals of the soft (low temperature) and hard (high temperature) domains. These two endothermal peaks are consistent with those described in a comprehensive evaluation of Bioflex® in the literature [25], which associates them to melting of soft and hard segments forming a thermoplastic copolyester-ether elastomer. In the first heating scans of irradiated specimens, the exothermal signal is observed to intensify and shift to a lower temperature with increasing radiation, as indicated by the values of peak temperature, T_{exo}, and related enthalpy, ΔH_{exo}, presented in table 4. For samples irradiated at 100 kGy and 140 kGy, diminished and less significant values of ΔH_{exo} are found due to the overlap of the signal with the endothermal melting peak of the hard segments. This anomaly can be ascribed to early degradation, as corroborated by the TGA signals (figure 8(c)), which indicate a significant degradation process that begins at lower temperatures (T_{onset} in table 4) in more irradiated systems, encompassing thermal zones analogous to those of the DSC exothermic signal; in particular, T_{onset} decreases by 10 °C for the lowest dose (45 kGy) and by up to 80 °C for the highest (992 kGy). Conversely, in the second heating scan, no substantial effects are closely associated with the absorbed dose, and both melting temperatures (T_{m1} and T_{m2}, corresponding to the soft and hard domains, respectively) and enthalpies (ΔH_{m1} and ΔH_{m2}) remain constant upon irradiation, except for minor changes

in the traces of the specimens that received the highest doses (910 kGy and 990 kGy); these two systems exhibit a slight decrease in ΔH_{m1}, and thus of the soft domain crystallinity, and a reduction of about 20 °C in T_{m2}, suggesting the formation of lower-quality hard domain crystals (see table 4). Concerning DMA results, all TPE systems exhibit a similar behaviour, characterised initially by a smooth modulus reduction between −50 °C and 0 °C, attributed to the melting of crystalline soft domains, and subsequently by an extended, gently sloped plateau that ultimately reveals a downward deviation, indicating the entrance in the flow regime upon the initial melting of the hard domain crystals. The temperature at which this deviation occurs, indicated in table 4 as T_{flow}, decreases as the absorbed dose increases. Specifically, irradiated specimens may be ranked into three groups depending on how the dose influences their behaviour with respect to the non-irradiated material:

- for dose values up to 100 kGy, the storage modulus curves of the specimens and their transition into the flow regime remain unaltered by irradiation;
- for dose values ranging from 100 kGy to 300 kGy, the onset of the flow regime appears to be marginally diminished (by no more than 10 °C);
- for the highest dose values (910 kGy and 990 kGy), a remarkable decrease in T_{exo} is observed (20 °C for 990 kGy; 30 °C for 910 kGy); in addition, the storage modulus at a specific temperature seems to be reduced, consistently with the reduction in the Young's modulus measured by tensile tests at room temperature.

3.3. Spectroscopy results

FTIR spectra of non-irradiated filaments were overall consistent with those found in literature [25, 30, 31]. After irradiation, all the materials show signs of oxidation, as revealed by the presence of a broad band around 3100–3600 cm^{-1}, associated to O–H stretching vibration. The remaining part of the spectra displayed no changes in the position of peaks and minor changes in the intensity of the signals, indicating no substantial changes in the chemistry of the filaments.

Raman spectroscopy on the three printing materials provided spectra that are also in agreement with the ones found in literature [25, 30, 32]. All the presented spectra have been normalised by the total area of Raman peaks, and are shown for different doses in figure 9.

ABS and TPE spectra did not evidence clear variations in the position of peaks and relative intensity in function of the dose, while we observed an increase in the fluorescence background of the spectrum with the absorbed dose. For the ABS we additionally report a broadening of the peak at 1600 cm^{-1}, that corresponds to the skeletal vibration of the C=C aromatic ring [32].

We did not observe significant differences on the spectrum in function of the sampling position along the radius of the filament for the ABS, but for the TPE irradiated at high doses we systematically observe an increase in the background along the radius of the filament (higher background near the surface of the filament), as shown in figure 10.

For what concerns PLA, we noticed a low repeatability of the spectrum in terms of fluorescence background, but still we did not observe new features on the spectra.

4. Discussion

The substantial changes in mechanical properties rather than chemical and thermal ones support the hypothesis of chain scission as the main radiation-induced effect for the three analysed materials, as discussed in the following.

PLA shows a significant decline in mechanical properties as a function of x-ray dose: non-irradiated samples undergo plastic deformation up to large strain values, but already at the lowest explored dose (45 kGy) brittle failure of the specimens is reported, and at 144 kGy the degradation is so severe that specimens cannot be even tested. These effects are similar to those observed in literature for gamma-irradiated PLA [11, 31]. More precisely, the authors of these studies managed to test specimens irradiated up to 150 kGy [11] or even 300 kGy [31] but, from doses of 100 kGy upwards, the strain at break they measured was never higher than 1% and the TS was reduced by 50% or more, thus confirming drastic embrittlement above 100 kGy. The different dose threshold for tensile test feasibility with respect to the present work may be attributed to differences in their experimental setup and irradiation conditions (i.e. different radiation type, dose rate, strain rate, sample geometry). Thermal examination by DSC yields minimal but noteworthy insights into the effects of radiation on PLA. The reduction in T_g and T_m, the slight decrease in ΔH_m, and the disappearing of the cold crystallisation peak observed for the most irradiated sample (144 kGy) may be attributed to a decrease in the molecular weight of the chains. Specifically, the increased presence of shorter chains may facilitate a plasticizing effect on T_g, it may diminish the quantity and quality of the crystals, and it may help in achieving complete crystallisation after cooling, so that no

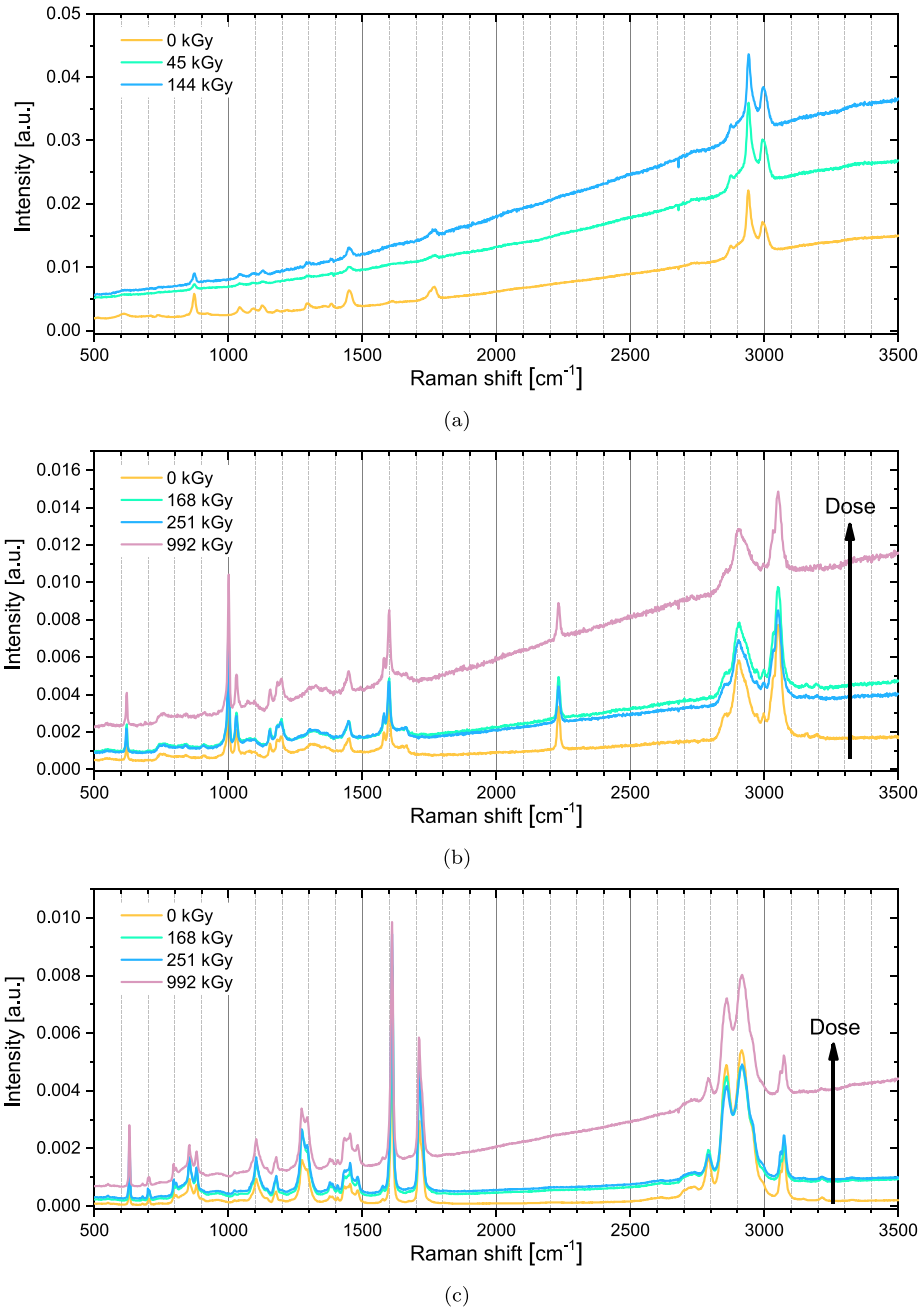

Figure 9. Raman normalised spectra for (a) PLA, (b) ABS and (c) TPE filaments.

recrystallisation is found in the second heating scan. Moreover, the reduction in both T_g and T_m is in line with what observed in the literature for PLA subjected to gamma irradiation [11, 31, 33]. Concerning the melting enthalpy, gamma-irradiated specimens also showed a slight reduction of ΔH_m for doses up to 150 kGy, whereas higher doses were found to invert this trend [33]. Finally, the moderate alteration in TGA traces has also been documented in the literature [11, 31] for PLA irradiated with ^{60}Co gamma rays up to 400 kGy, revealing a slight increase in mass loss during the initial degradation phase for samples irradiated at higher dose. This was attributed to chain scission resulting from the accumulation of thermally labile peroxy groups in PLA, which decompose upon heating [34]. The hypothesis of chain scission as prevalent irradiation effect is also in agreement with the observed degradation of mechanical properties.

The tensile properties of the ABS filament remain stable for dose levels up to 300 kGy, but significant alterations occur at higher doses ranging from 1 to 2 MGy. Tensile tests evidence a radiation-induced transition from a ductile to a brittle behaviour, associated to a decrease of both TS and ϵ_b, while E remains constant, consistently with findings reported in the literature for ABS subjected to gamma irradiation with doses below 1 MGy [6, 31]. Eventually, samples irradiated at 1900 kGy become untestable. Also in this case, DSC and TGA traces offer limited insights into the structural evolution of ABS. T_g remains unchanged, while

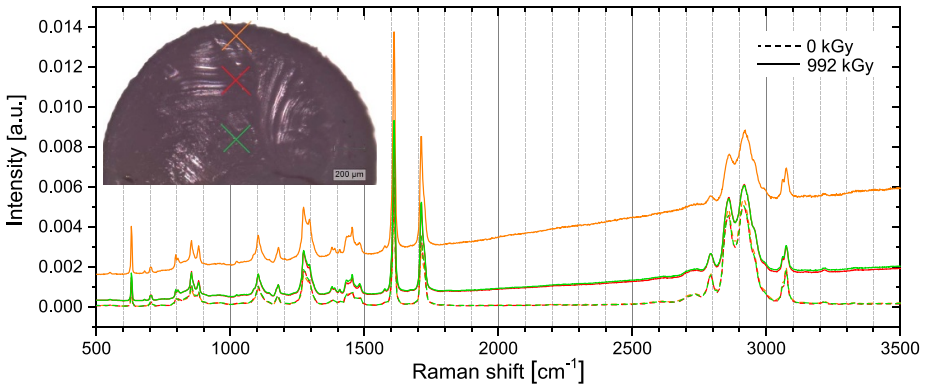

Figure 10. Raman spectra for non-irradiated (dotted lines) and irradiated (at 992 kGy, solid lines) TPE filament in function of the position along the radius of the filament.

a slight decrease of T_{onset} and T_{peak} is observed as the dose increases. The latter phenomenon is also documented in the literature, where it has been attributed to the facile volatilisation of low molecular weight fragments generated during high-dose irradiation (2.68 MGy, gamma rays) [31]. Importantly, the DMTA results in the present work reveal a shortening of the rubbery plateau in function of the dose, indicating a gradual decrease in molecular weight upon x-ray irradiation. In fact, the extension of the rubbery plateau is generally associated with the molecular weight of the polymer: elongated molecular chains tend to prolong the rubbery plateau and defer the transition into the flow regime due to an increased entanglement of longer chains. This suggests the predominance of chain scission rather than crosslinking at x-ray irradiation of ABS up to 1 MGy, which is also consistent with the constant trend found for the Young's modulus, showing no radiation-induced stiffening. By contrast, the effects of gamma irradiation on ABS have been associated in the literature [31] with crosslinking, because of stiffening observed at high doses (from 1 MGy upwards). However, the increase in Young's modulus in gamma-irradiated ABS was accompanied by a remarkable decrease in TS, which may be ascribed to chain scission. Because of this and of the differences in the explored dose levels, there is no sufficient evidence to claim a different effect of x-rays and gamma rays on ABS. Concerning Raman analyses, the increase in the spectrum background is related to the fluorescence of the radicals formed during the irradiation. In addition, the broadening of the peak at 1600 cm^{-1} suggests the formation of additional carbonyl groups as reported in literature [31].

The most relevant radiation-induced effect on the mechanical properties is observed for the TPE, which evolves from the possibility to withstand deformations above 800% to extremely brittle conditions around 1 MGy. Beyond 250 kGy, a noticeable decrease in E, TS, and ϵ_b becomes evident as the absorbed dose increases. According to DSC analyses, the crystalline domains of TPE are not affected by irradiation if not for dose values around 1 MGy, slightly reducing the soft domain crystallinity and the quality of hard domain crystals. Conversely, the thermal stability of this material appears strongly influenced, as results from TGA and DSC indicate a significant degradation process that begins at lower temperatures in more irradiated systems. Moreover, the temperature at which TPE enters the flow regime decreases with dose, as shown from the DMTA for dose values above 100 kGy.

Importantly, this progressive shift may indicate a decrease in molecular weight due to chain scission phenomena, which would be consistent with the reduction of strength and ductility highlighted by mechanical tests. In addition, when the dose reaches the highest values (approximately 1 MGy) a decrease in stiffness is also reported, both in terms of Young's modulus and in terms of storage modulus. This may be attributed to the cracks which appeared on the surface of the filaments after irradiation at such high doses, significantly altering the specimens' geometry. Finally, an increase in the fluorescence background in the Raman spectrum is also observed for TPE after irradiation. Notably, the increase in the fluorescence is more pronounced near the surface of the filament, suggesting potential oxygenation effects—which depend on material porosity, sample geometry etc—that impact on radical formation, and thus on the sample damage. This aligns with the presence of superficial cracks observed on the TPE filament irradiated at higher doses. However, the increased oxygenation could also be a consequence of these superficial cracks rather than their cause, highlighting the need for further investigations to clarify the relationship between oxygenation and structural damage.

5. Conclusions

Results of the irradiation campaign evidence a progressive degradation of the properties of the tested materials with dose, prevalently regarding the mechanical properties rather than the chemical and thermal ones. The findings may be consistently correlated with chain scission as the main damage mechanism.

The geometry of the samples may influence the results, as suggested by the spectroscopic analysis of TPE. Oxygenation seems to induce a more pronounced damage, implying that the degradation observed in filaments may differ from that in printed objects. This difference arises from the varying dynamics of oxygen diffusion within the material, which depend on factors such as sample thickness, surface area, porosity, and other geometric characteristics.

The collected data allow the different materials to be compared, providing useful information for the selection of the most radiation tolerant ones. Among the three materials, PLA exhibits the lowest radiation tolerance, with a dramatic reduction in TS occurring beyond 100 kGy. In contrast, TPE and ABS demonstrate significantly higher radiation resistance, reaching comparable levels of mechanical degradation only after exposure to 1 MGy and 2 MGy, respectively. Future experimental campaigns will focus on the dependence of radiation effects on other parameters, such as temperature and environmental atmosphere, as well as the effects of the geometry of the sample and dose rate to further investigate oxygenation effects. Preliminary results on samples irradiated at 0.2 Gy s^{-1} revealed no significant differences compared to 0.6 Gy s^{-1}, therefore a significantly different dose rate will be investigated by exposing samples to a 2.5 MeV electron beam (>10 MGy h^{-1}).

Data availability statement

All data that support the findings of this study are included within the article (and any supplementary information files).

Acknowledgments

The authors wish to thank F Bignotti (University of Brescia, Italy), F Vocanson and M Royon (Universite Jean Monnet Saint-Etienne, France) for the FTIR measurements, and Y Q Aguiar (CERN) for the RPL dosimeter readings. The work of L Sostero was co-funded by the European Union (Piano Nazionale di Ripresa e Resilienza—Next Generation EU—Decreto Ministeriale 352/2022). The work of M Ferrari was supported by the French Agence Nationale de la Recherche PROJET N° ANR-22-CPJ2-0117-01.

ORCID iDs

L Sostero https://orcid.org/0000-0002-8322-2973
M Ferrari https://orcid.org/0000-0002-2447-9365
D Pagano https://orcid.org/0000-0003-0333-448X
S Pandini https://orcid.org/0000-0003-2390-8495
C Pasini https://orcid.org/0000-0001-7478-239X
S Girard https://orcid.org/0000-0002-9804-8971

References

[1] Jones A R *et al* 2016 On the design of a remotely-deployed detection system for reactor assessment at Fukushima Daiichi *2016 IEEE Nuclear Science Symp., Medical Imaging Conf. and Room-Temperature Semiconductor Detector Workshop (NSS/MIC/RTSD)* (IEEE)
[2] Martin H, Watson S, Lennox B and Poteau X 2018 Miniature inspection robot for restricted access exploration (mirrax) *WM Symposia* vol 2018
[3] Wangsgard W and Winters M 2018 Validation of a sterilization dose for products manufactured using a 3D printer *Radiat. Phys. Chem.* **143** 38–40
[4] Rynio P, Galant K, Wójcik Ł, Grygorcewicz B, Kazimierczak A, Falkowski A, Gutowski P, Dołegowska B and Kawa M 2022 Effects of sterilization methods on different 3D printable materials for templates of physician-modified aortic stent grafts used in vascular surgery—a preliminary study *Int. J. Mol. Sci.* **23** 3539
[5] Horst F, Beyreuther E, Bodenstein E, Gantz S, Misseroni D, Pugno N M, Schuy C, Tommasino F, Weber U and Pawelke J 2023 Passive sobp generation from a static proton pencil beam using 3D-printed range modulators for flash experiments *Front. Phys.* **11** 1213779
[6] Rankouhi B, Delfanian F, McTaggart R and Letcher T 2016 An experimental investigation of the effects of gamma radiation on 3D printed abs for in-space manufacturing purposes *Advances in Aerospace Technology, IMECE2016 (American Society of Mechanical Engineers)* vol 1
[7] McGuire T, Hirsch M, Parsons M, Leake S and Straub J 2016 Design for an in-space 3D printer *Proc. SPIE* **9838** 256–65
[8] Coenen S 1995 Radiation Effects on Polymers, SCK CEN
[9] Bolt R and Carroll J 1963 *Radiation Effects on Organic Materials* (Academic)

[10] Hasan M K, Staack D, Pillai S D, Fifield L S and Pharr M 2024 Connecting radiation-driven changes in structural, thermal and mechanical properties in several medical device polymers *Polym. Degrad. Stab.* **221** 110677
[11] West C, McTaggart R, Letcher T, Raynie D and Roy R 2019 Effects of gamma irradiation upon the mechanical and chemical properties of 3D-printed samples of polylactic acid *J. Manuf. Sci. Eng.* **141** 041002
[12] Rankouhi B, Javadpour S, Delfanian F, McTaggart R and Letcher T 2018 Experimental investigation of mechanical performance and printability of gamma-irradiated additively manufactured abs *J. Mater. Eng. Perform.* **27** 3643–54
[13] Schmalzer A M, Cady C M, Geller D, Ortiz-Acosta D, Zocco A T, Stull J and Labouriau A 2017 Gamma radiation effects on siloxane-based additive manufactured structures *Radiat. Phys. Chem.* **130** 103–11
[14] Croonenborghs B, Smith M and Strain P 2007 X-ray versus gamma irradiation effects on polymers *Radiat. Phys. Chem.* **76** 1676–8
[15] Fintzou A T, Kontominas M G, Badeka A V, Stahl M R and Riganakos K A 2007 Effect of electron-beam and gamma-irradiation on physicochemical and mechanical properties of polypropylene syringes as a function of irradiation dose: study under vacuum *Radiat. Phys. Chem.* **76** 1147–55
[16] Scagliusi S R, Cardoso E L and Lugao A B 2012 Effect of gamma radiation on chlorobutyl rubber vulcanized by three different crosslinking systems *Radiat. Phys. Chem.* **81** 1370–3
[17] Abdel Tawab K, Ibrahim S M and Magida M M 2012 The effect of gamma irradiation on mechanical and thermal properties of recycling polyethylene terephthalate and low density polyethylene (R-PET/LDPE) blend compatibilized by ethylene vinyl acetate (EVA) *J. Radioanal. Nucl. Chem.* **295** 1313–9
[18] Buttafava A, Consolati G, Mariani M, Quasso F and Ravasio U 2005 Effects induced by gamma irradiation of different polyesters studied by viscometry, thermal analysis and positron annihilation spectroscopy *Polym. Degrad. Stab.* **89** 133–9
[19] Youm J S, Kim J C and Yang K S 2012 Elastic property of polyolefin elastomer film cross linked by electron beam irradiation *Fibers Polym.* **13** 1165–9
[20] Manas D, Ovsik M, Mizera A, Manas M, Hylova L, Bednarik M and Stanek M 2018 The effect of irradiation on mechanical and thermal properties of selected types of polymers *Polymers* **10** 158
[21] Giacomazzi L, Girard S, Martin-Samos L, Boukenter A, Ouerdane Y, Paillet P, Richard N, Marcandella C 2015 Radiation effects on optical fibers and fiber-based sensors.
[22] Lunt J 1998 Large-scale production, properties and commercial applications of polylactic acid polymers *Polym. Degrad. Stab.* **59** 145–52
[23] Dey A, Roan Eagle I N and Yodo N 2021 A review on filament materials for fused filament fabrication *J. Manuf. Mater. Process.* **5** 69
[24] Pious C and Thomas S 2016 *Polymeric Materials—Structure, Properties and Applications* (Elsevier) pp 21–39
[25] Haryńska A, Carayon I, Kosmela P, Szeliski K, Łapiński M, Pokrywczyńska M, Kucińska-Lipka J and Janik H 2020 A comprehensive evaluation of flexible FDM/FFF 3D printing filament as a potential material in medical application *Eur. Polym. J.* **138** 109958
[26] Awasthi P and Banerjee S S 2021 Fused deposition modeling of thermoplastic elastomeric materials: challenges and opportunities *Addit. Manuf.* **46** 102177
[27] Poludniowski G, Omar A, Bujila R and Andreo P 2021 Technical note: SpekPy v2.0—a software toolkit for modeling x-ray tube spectra *Med. Phys.* **48** 3630–7
[28] Sato T *et al* 2018 Features of particle and heavy ion transport code system (PHITS) version 3.02 *J. Nucl. Sci. Technol.* **55** 684–90
[29] Luo R, Kang D, Huang C, Yan T, Li P, Ren H and Zhang Z 2023 Mechanical properties, radiation resistance performances and mechanism insights of nitrile butadiene rubber irradiated with high-dose gamma rays *Polymers* **15** 3723
[30] Pandele A M, Constantinescu A, Radu I C, Miculescu F, Ioan Voicu S and Ciocan L T 2020 Synthesis and characterization of pla-micro-structured hydroxyapatite composite films *Materials* **13** 274
[31] Wady P, Wasilewski A, Brock L, Edge R, Baidak A, McBride C, Leay L, Griffiths A and Vallés C 2020 Effect of ionising radiation on the mechanical and structural properties of 3D printed plastics *Addit. Manuf.* **31** 100907
[32] Petousis M, Michailidis N, Papadakis V M, Korlos A, Mountakis N, Argyros A, Dimitriou E, Charou C, Moutsopoulou A and Vidakis N 2023 Optimizing the rheological and thermomechanical response of acrylonitrile butadiene styrene/silicon nitride nanocomposites in material extrusion additive manufacturing *Nanomaterials* **13** 1588
[33] Madera-Santana T J, Meléndrez R, González-García G, Quintana-Owen P and Pillai S D 2016 Effect of gamma irradiation on physicochemical properties of commercial poly(lactic acid) clamshell for food packaging *Radiat. Phys. Chem.* **123** 6–13
[34] Babanalbandi A, Hill D, Hunter D and Kettle L 1999 Thermal stability of poly(lactic acid) before and after γ-radiolysis *Polymer Int.* **48** 980–4